Guo et al. Alzheimer's Research & Therapy (2020) 12:97
https://doi.org/10.1186/s13195-020-00665-8

Alzheimer's Research & Therapy

RESEARCH Open Access

Normalization of CSF pTau measurement by $A\beta_{40}$ improves its performance as a biomarker of Alzheimer's disease

Tengfei Guo[1,2*], Deniz Korman[1], Renaud La Joie[3], Leslie M. Shaw[4], John Q. Trojanowski[4], William J. Jagust[1,2], Susan M. Landau[1,2] and for the Alzheimer's Disease Neuroimaging Initiative

Abstract

Background: Alzheimer's disease (AD)-related tauopathy can be measured with CSF phosphorylated tau (pTau) and tau PET. We aim to investigate the associations between these measurements and their relative ability to predict subsequent disease progression.

Methods: In 219 cognitively unimpaired and 122 impaired Alzheimer's Disease Neuroimaging Initiative participants with concurrent amyloid-β (Aβ) PET (^{18}F-florbetapir or ^{18}F-florbetaben), ^{18}F-flortaucipir (FTP) PET, CSF measurements, structural MRI, and cognition, we examined inter-relationships between these biomarkers and their predictions of subsequent FTP and cognition changes.

Results: The use of a CSF pTau/$A\beta_{40}$ ratio eliminated positive associations we observed between CSF pTau alone and CSF $A\beta_{42}$ in the normal Aβ range likely reflecting individual differences in CSF production rather than pathology. Use of the CSF pTau/$A\beta_{40}$ ratio also increased expected associations with Aβ PET, FTP PET, hippocampal volume, and cognitive decline compared to pTau alone. In Aβ+ individuals, abnormal CSF pTau/$A\beta_{40}$ only individuals (26.7%) were 4 times more prevalent ($p < 0.001$) than abnormal FTP only individuals (6.8%). Furthermore, among individuals on the AD pathway, CSF pTau/$A\beta_{40}$ mediates the association between Aβ PET and FTP PET accumulation, but FTP PET is more closely linked to subsequent cognitive decline than CSF pTau/$A\beta_{40}$.

Conclusions: Together, these findings suggest that CSF pTau/$A\beta_{40}$ may be a superior measure of tauopathy compared to CSF pTau alone, and CSF pTau/$A\beta_{40}$ enables detection of tau accumulation at an earlier stage than FTP among Aβ+ individuals.

Keywords: Tau, CSF pTau/$A\beta_{40}$, PET, Cognition, Alzheimer's disease

* Correspondence: tengfei.guo@berkeley.edu
[1]Helen Wills Neuroscience Institute, University of California, 132 Barker Hall, Berkeley, CA 94720, USA
[2]Molecular Biophysics and Integrated Bioimaging, Lawrence Berkeley National Laboratory, Berkeley, CA, USA
Full list of author information is available at the end of the article

© The Author(s). 2020 **Open Access** This article is licensed under a Creative Commons Attribution 4.0 International License, which permits use, sharing, adaptation, distribution and reproduction in any medium or format, as long as you give appropriate credit to the original author(s) and the source, provide a link to the Creative Commons licence, and indicate if changes were made. The images or other third party material in this article are included in the article's Creative Commons licence, unless indicated otherwise in a credit line to the material. If material is not included in the article's Creative Commons licence and your intended use is not permitted by statutory regulation or exceeds the permitted use, you will need to obtain permission directly from the copyright holder. To view a copy of this licence, visit http://creativecommons.org/licenses/by/4.0/. The Creative Commons Public Domain Dedication waiver (http://creativecommons.org/publicdomain/zero/1.0/) applies to the data made available in this article, unless otherwise stated in a credit line to the data.

Background

Extracellular amyloid-β (Aβ) peptides in cortical Aβ plaques and intracellular phosphorylated tau protein as neurofibrillary tangles are key hallmarks of Alzheimer's disease (AD) that can be measured in vivo with positron emission tomography (PET) imaging and biofluid markers including plasma and cerebrospinal fluid (CSF) assays. The relationship between CSF Aβ and Aβ PET in AD has been widely reported [1–8], but relationships between CSF tau and tau PET are uncertain [9–13]. Recent studies reported that individuals with abnormal CSF phosphorylated tau (pTau) were more prevalent than individuals with abnormal tau PET only [14], and that abnormal tau PET but not CSF pTau was related to cognitive decline [15], suggesting that CSF and PET may not be interchangeable indices of tau pathology.

There are also remaining technical questions involved in measurement of CSF biomarkers. Elevated (abnormal) CSF pTau has been observed in cases with exceptionally elevated CSF $A\beta_{42}$ in the Aβ− range [7, 16]. Positive correlations between these measurements in the Aβ− range are likely not AD-related but are instead due to individual variability in CSF production. This would suggest that abnormal CSF pTau in individuals with elevated CSF $A\beta_{42}$ lack a pathological basis and instead reflect disease-invariant CSF increases that would be observed across all CSF markers. To address this phenomenon, use of the CSF $A\beta_{42}/A\beta_{40}$ ratio has been proposed over CSF $A\beta_{42}$ alone [6, 7, 17–19], since $A\beta_{40}$ is most abundant Aβ species in CSF [19, 20], and expected to increase due to higher overall Aβ production but not sensitive to AD [21–29]. We hypothesize that a similar adjustment of CSF pTau using CSF $A\beta_{40}$ may reduce noise and improve associations with other biomarkers.

In this study, we used Alzheimer's Disease Neuroimaging Initiative (ADNI) participants to explore the utility of a CSF $pTau/A\beta_{40}$ ratio to reduce noise in pTau measurements and improve associations with downstream markers of AD progression. We then examined the biological plausibility of this biomarker in relation to regional ^{18}−Flortaucipir (FTP) PET as well as subsequent tau PET and cognitive changes.

Methods

Participants

Data used in this study were obtained from the ADNI database (ida.loni.usc.edu; specific datasets used in this study are named below). The ADNI study was approved by institutional review boards of all participating centers, and written informed consent was obtained from all participants or their authorized representatives. In total, 219 cognitively unimpaired (CU) elderly adults, 91 mild cognitive impairment (MCI), and 31 AD patients with concurrent (acquisition interval within 1 year) Aβ PET (^{18}F-florbetapir (FBP) or ^{18}F-florbetaben (FBB)), CSF $A\beta_{40}$, $A\beta_{42}$ and $pTau_{181}$, FTP tau PET, structural MRI, and cognitive test were included in this study.

PET and MRI imaging

PET data was acquired in 5-min frames from 50 to 70 min (FBP), 90–110 min (FBB), and 75–105 min (FTP) post-injection (http://adni-info.org). PET and structural MRI scans were downloaded from the Laboratory of NeuroImaging (LONI) (ida.loni.usc.edu) and processed with Freesurfer V5.3.0. All fully pre-processed PET scans were co-registered to the structural MRI scan that was closest in time to the baseline PET. Regions of interest (ROIs) were defined on each structural MRI scan using Freesurfer (V5.3.0) and used to extract regional FBP, FBB, and FTP measurements from the co-registered PET images as described previously [30, 31].

Briefly, FBP or FBB standardized uptake value ratios (SUVRs) were calculated by dividing frontal, cingulate, parietal, and temporal regional uptake to that in the whole cerebellum to generate COMPOSITE SUVRs [30]. COMPOSITE SUVRs for FBP ≥1.11 or FBB ≥1.08 were defined as Aβ+ as described on the ADNI website. Aβ positivity was defined by Aβ PET in this study. FBP (UCBERKELEYAV45_05_12_20.csv) and FBB (UCBERKELEYFBB_05_12_20.csv) SUVRs were converted to Centiloids using the equations $Centiloid = (196.9 \times SUVR_{FBP}) - 196.03$ for FBP and $Centiloid = (159.08 \times SUVR_{FBB}) - 151.65$ for FBB (ADNI_Centiloid_Methods_Instruction_20181113.pdf in LONI website (ida.loni.usc.edu)).

For FTP (BERKELEYAV1451_05_12_20.csv), composite Temporal-metaROI (including entorhinal, parahippocampal, fusiform, amygdala, inferior temporal, and middle temporal) [32] and entorhinal cortex SUVRs were calculated using inferior cerebellar cortex intensity normalization [31]. To define FTP SUVR thresholds, we carried out ROC analyses with Temporal-metaROI and entorhinal SUVR values using the Youden index classifying 280 Aβ PET− ADNI CU participants and 183 Aβ PET+ ADNI MCI and AD patients as the endpoint (Supplemental Figs. 1–4). This resulted in a threshold of 1.25 for the Temporal-metaROI and 1.21 for entorhinal cortex. Among these 463 ADNI participants for the definition of tau PET cutoffs, 217 (47%) participants were included in the following analyses of this study. We also examined alternative thresholds for these regions defined by the mean + 2SD of 280 Aβ PET- ADNI CU participants. These resulted in more conservative thresholds of 1.34 for the Temporal-metaROI and 1.31 for entorhinal cortex. In total, 34% of 341 participants had longitudinal FTP data. FTP slope (ΔFTP, SUVR units per year) was calculated based on longitudinal FTP data for each individual using linear mixed effects (LME) model, including

the following independent variables: time, APOE-ε4 status, age and gender, and a random slope and intercept. Since white matter intensity normalization has shown less variability for longitudinal tau PET changes [33–35], we calculated FTP slopes using a white matter reference region.

Hippocampal volume (HCV) (mm^3) was calculated across hemispheres from the structural MRI scan that was closest in time to the baseline PET scan and for subsequent MRI scans using Freesurfer, and adjusted by estimated intracranial volume (ICV) using the regression approach [36]: adjusted HCV (aHCV) = HCV − 0.0017 × (ICV − 1 498858), where 0.0017 and 1498858 represent the correlation coefficient between HCV and ICV, and the mean of ICV in Aβ− 323 ADNI CU participants. In total, 41% of 341 participants had longitudinal aHCV data. aHCV slope (ΔaHCV, mm^3 units per year) was calculated based on longitudinal aHCV data for each individual using LME model, including the following independent variables: time, APOE-ε4 status, age, gender and education, and a random slope and intercept.

CSF $Aβ_{40}$, $Aβ_{42}$, and pTau

CSF $Aβ_{40}$, $Aβ_{42}$, and pTau were analyzed by the University of Pennsylvania ADNI Biomarker core laboratory using the fully automated Roche Elecsys and cobas e 601 immunoassay analyzer system [16, 37]. CSF data (UPENNBIOMK10_07_29_19.csv) were downloaded from ADNI website. A threshold for abnormal CSF pTau was defined as ≥22 pg/mL based on an ROC analysis using the Youden index classifying 320 Aβ PET− ADNI CU participants and 429 Aβ PET+ ADNI MCI and AD patients as the endpoint (Supplemental Figs. 5–6). We also defined an alternative threshold of ≥31 for CSF pTau which was based on the mean + 2SD of CSF pTau in 320 Aβ PET− ADNI CU participants. We calculated the CSF pTau/$Aβ_{40}$ ratio threshold as ≥0.0012 according to the same ROC approach classifying 169 Aβ PET− CU participants and 161 Aβ PET+ MCI and AD patients as the endpoint (Supplemental Figs. 7–8), and the alternative threshold was ≥0.0014 based on the mean + 2SD of the CSF pTau/$Aβ_{40}$ ratio in 169 Aβ PET− ADNI CU participants. Among these 749 ADNI participants for the definition of CSF pTau, 212 (28%) participants were included in the following analyses of this study. Among these 329 ADNI participants for the definition of CSF pTau/$Aβ_{40}$, 201 (61%) participants were included in the following analyses of this study.

Cognition

The Delayed Recall portion of the Alzheimer's Disease Assessment Scale (ADASSCORES.csv and ADAS_ADNIGO23.csv downloaded at April 28, 2020), the delayed recall score on the logical memory IIa subtest from the Wechsler Memory Scale, the digit symbol substitution test score from the Wechsler Adult Intelligence Scale–Revised (NEUROBAT.csv downloaded at April 28, 2020), and the MMSE total score (MMSE.csv downloaded at April 28, 2020) were transferred to standard z scores (using the mean values of ADNI CU participants). Preclinical Alzheimer Cognitive Composite (PACC) scores [38] were calculated by combining these 4 cognitive z scores to one composite score. In total, 59% of 341 participants had longitudinal PACC data. PACC slope (ΔPACC) was calculated for each participant based on longitudinal PACC scores using LME model, including the following independent variables: time, APOE-ε4 status, age, gender and education, and a random slope and intercept.

Statistical analysis

Normality of distributions was tested using the Shapiro-Wilk test and visual inspection of data. Data are presented as median (interquartile range (IQR)) or number (%). Baseline characteristics were compared between Aβ− and Aβ+ groups by using a two-tailed Mann-Whitney test or Fisher's exact test.

In order to evaluate the feasibility of using CSF pTau/$Aβ_{40}$ as an alternative to CSF pTau, we first used generalized linear models (GLM) to examine the relationships of CSF $Aβ_{40}$ with Aβ PET and tau PET to confirm that CSF $Aβ_{40}$ is not related to AD biomarkers, and subsequently investigated the cross-sectional associations between CSF $Aβ_{42}$, pTau and pTau/$Aβ_{40}$, and controlling for APOE-ε4 status, diagnosis, sex, and age. A false discovery rate of 0.05 using the Benjamini-Hochberg approach was employed for 35 regions.

The slopes of FTP SUVR, aHCV, and PACC post baseline CSF collection were calculated using LME models over time from the first measurement point post baseline CSF collection (time = 0) to the last measurement point for each participant. The time variable is anchored to the baseline CSF measurement. In order to study whether elevated CSF pTau/$Aβ_{40}$ is more related to the progression of AD than high CSF pTau, we also used GLM models to investigate the associations of CSF pTau and pTau/$Aβ_{40}$ with Aβ PET, tau PET, aHCV, ΔaHCV, PACC, and ΔPACC, controlling for APOE-ε4 status, diagnosis, sex, age, and education. Since there was a time difference between baseline CSF collection point and the first measurements of FTP SUVR, aHCV, and PACC post baseline CSF collection, we included these time differences in the GLM models. Because we found use of the CSF pTau/$Aβ_{40}$ ratio abolished the positive correlation between CSF pTau and $Aβ_{42}$ among Aβ PET− range (see Fig. 1c, d in "Results") and improved the associations with Aβ PET, tau PET, aHCV,

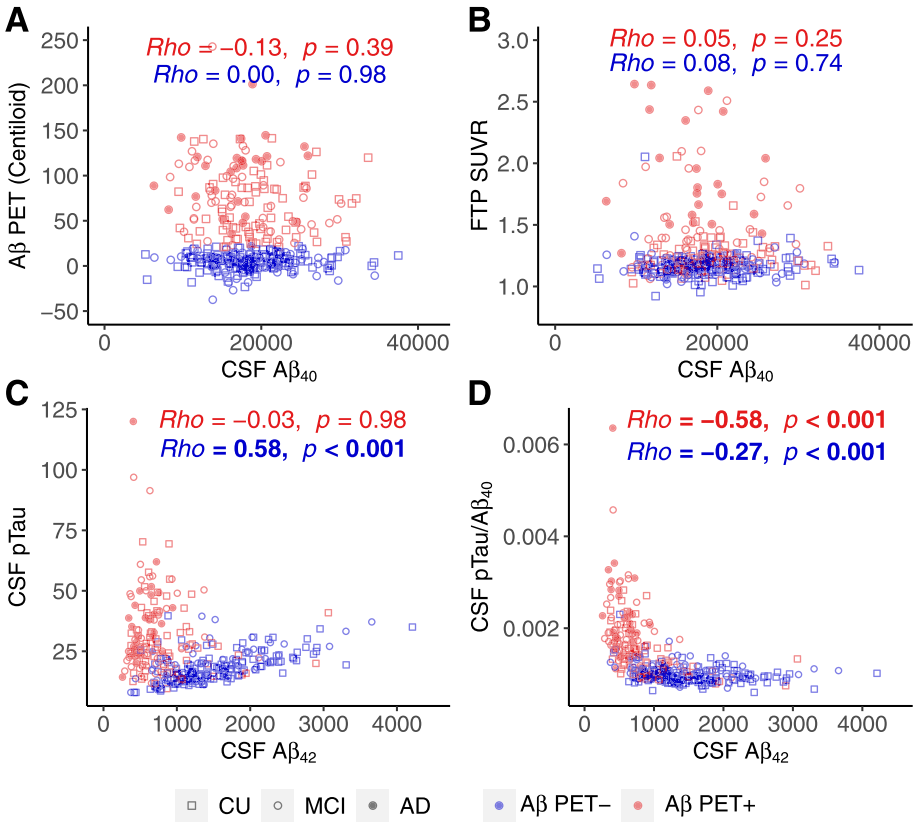

Fig. 1 Cross-sectional associations between CSF $A\beta_{42}$, pTau, and pTau/$A\beta_{40}$. Associations of **a** Aβ PET (Centiloid) and **b** tau PET (Temporal-metaROI FTP SUVR) with CSF $A\beta_{40}$. Associations between CSF $A\beta_{42}$ and **c** CSF pTau and **d** CSF pTau/$A\beta_{40}$. The horizontal gray dashed lines reflect the abnormal thresholds of corresponding biomarkers on *y*-axis. Abbreviations: pTau = phosphorylated tau; Aβ = amyloid-β; FTP = ^{18}F-flortaucipir; CU = cognitively unimpaired; MCI = mild cognitive impairment; AD = Alzheimer's disease

ΔaHCV, PACC, and ΔPACC (see Fig. 2 in "Results"), we used this ratio in subsequent analyses.

We then explored the biological plausibility of the CSF pTau/$A\beta_{40}$ by examining associations between CSF pTau/$A\beta_{40}$ and FTP SUVRs in 35 Freesurfer-defined ROIs, controlling for Aβ PET (in Centiloids), APOE-ε4 status, diagnosis, sex, and age. Spearman's rho was calculated between CSF pTau/$A\beta_{40}$ and FTP SUVR. Subsequently, we examined the associations between Aβ PET, CSF pTau/$A\beta_{40}$, CSF pTau, and tau PET (entorhinal or Temporal-metaROI) in Aβ− and Aβ+ participants, controlling for APOE-ε4 status, diagnosis, sex, and age.

In order to investigate the predictive effect of baseline Aβ PET, CSF pTau/$A\beta_{40}$, and FTP on subsequent ΔFTP and ΔPACC, we used these variables at baseline to predict subsequent ΔFTP and ΔPACC in participants with longitudinal tau PET and PACC data respectively. In order to explore temporal relationships between Aβ and tau, we also examined the sequential associations between baseline Aβ PET, CSF pTau/$A\beta_{40}$ ratio, FTP, and ΔFTP in Aβ+ participants using latent variable modeling (R; Lavaan package) [39].

For GLM models with non-Gaussian distribution outcomes (Aβ and tau PET), we used a "log" link function in the Gaussian family to study the associations between predictor and outcome. Spearman's rank correlation coefficient (rho) was calculated between predictor and outcome. We selected $p < 0.05$ as the significance level. All statistical analyses were performed in the statistical program *R* (v3.6.2, The R Foundation for Statistical Computing).

Results

Demographics

Measurements were acquired between September 21, 2015 and April 9, 2020. Demographics can be found in Table 1. In total, 341 participants had contemporaneous CSF $A\beta_{40}$, $A\beta_{42}$ and pTau, Aβ PET, tau PET, structural MRI, and PACC cognitive score. At baseline, Aβ+ participants were significantly older and had greater CSF pTau, CSF pTau/$A\beta_{40}$ and Temporal-metaROI FTP SUVR, lower aHCV, lower cognitive test scores, and a higher percentage of APOE-ε4 carriers than Aβ− participants. Longitudinally, 116, 139, and 202 participants had

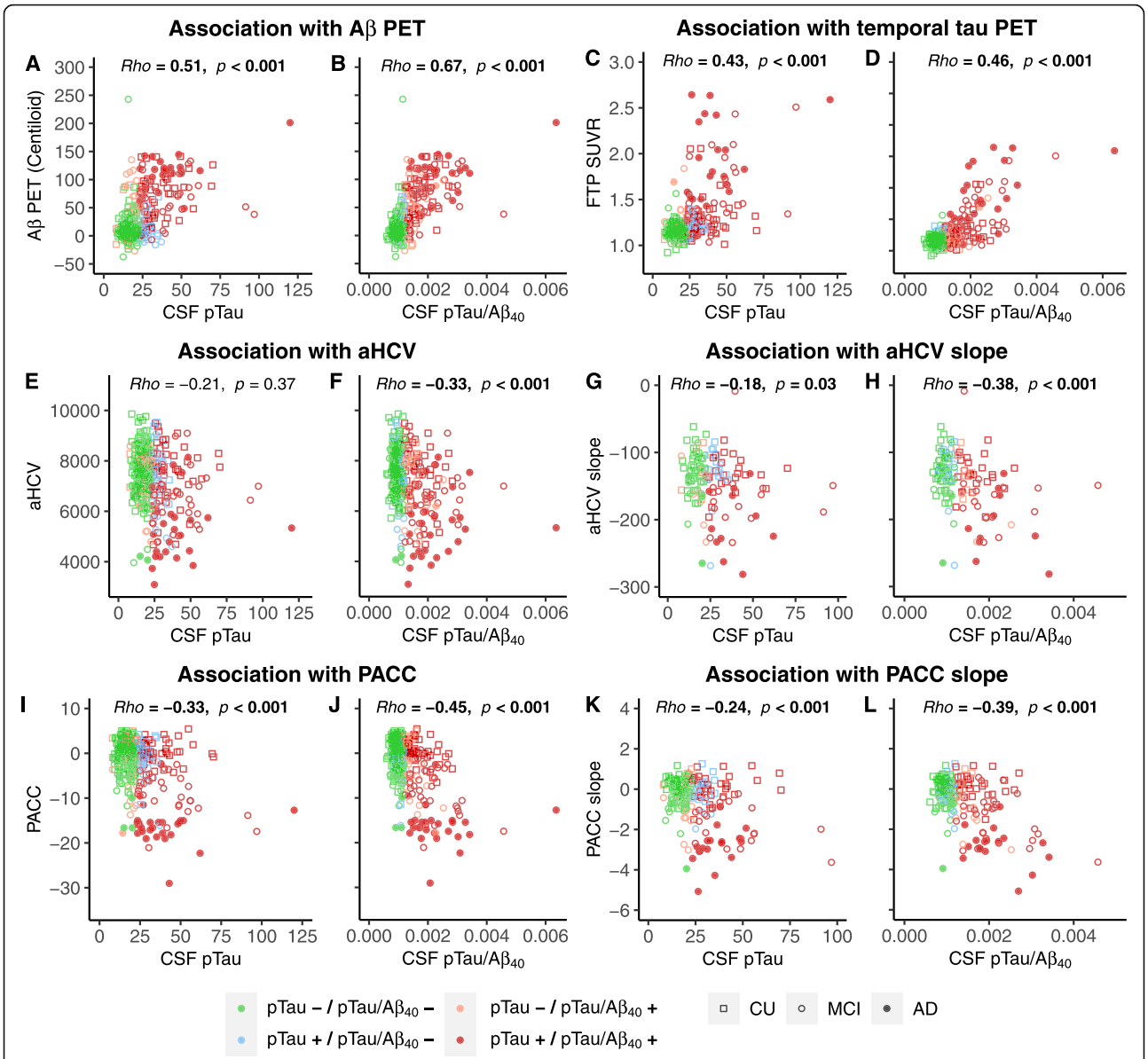

Fig. 2 Associations between CSF pTau and pTau/$A\beta_{40}$, Aβ PET, tau PET, neurodegeneration and cognition. Associations of baseline CSF pTau and pTau/$A\beta_{40}$ with baseline Aβ PET (**a**, **b**), baseline Temporal-metaROI FTP SUVR (**c**, **d**), baseline (**e**, **f**), and slope (**g**, **h**) of adjusted hippocampal volume (aHCV) (mm^3), baseline (**i**, **j**) and slope (**k**, **l**) of PACC cognitive score. Different colors reflect the concordance and discordance between CSF pTau and CSF pTau/$A\beta_{40}$. For example, pTau−/pTau/$A\beta_{40}$− indicates the individual was negative according to both CSF pTau and CSF pTau/$A\beta_{40}$, while pTau+/pTau/$A\beta_{40}$− indicates the individual was positive according to CSF pTau but negative according to CSF pTau/$A\beta_{40}$

> 2 FTP PET scans (median follow-up 1.2 (range 0.7–3.3) years), structural MRI scans (median follow-up 1.4 (range 0.8–3.8) years), and PACC cognitive scores (median follow-up 1.2 (range 0.7–4.0) years) respectively.

Use of CSF $A\beta_{40}$ to adjust CSF pTau

CSF $A\beta_{40}$ was not associated with Aβ PET or tau PET regardless of Aβ PET status (Fig. 1a, b). Before normalizing to CSF $A\beta_{40}$, CSF pTau was positively (standardized β (β_{std}) = 0.59[95% confidence interval (CI), 0.48, 0.71]) associated with CSF $A\beta_{42}$ in Aβ PET− participants, whereas no association was found in Aβ+ participants (Fig. 1c). We also verified that there was a similar positive association between CSF pTau and CSF $A\beta_{42}$ analyzed with mass spectrometry rather than the Roche Elecsys immunoassay in a partially overlapping (9.8%) sample of 384 Aβ− participants (Supplemental Fig. 9). After normalizing CSF pTau using CSF $A\beta_{40}$, CSF pTau/$A\beta_{40}$ was negatively (Fig. 1d) associated with CSF $A\beta_{42}$ in both Aβ− (β_{std} = − 0.27 [95% CI, − 0.41, − 0.13]) and Aβ+ (β_{std} = − 0.32 [95% CI, − 0.48, − 0.15]) participants.

Table 1 Characteristics of participants in this study

Aβ PET status	Aβ−	Aβ+	*p* value
341 participants with CSF $Aβ_{40}$, $Aβ_{42}$ and pTau, Aβ PET, and tau PET			
Sample size	195 (57%)	146 (43%)	
CU/MCI/AD	145/46/4	74/45/27	
Age (years)	70.4 (9.4)	74.7 (10.4)	**< 0.001**
Education (years)	18 (2)	16 (3)	0.07
Female (%)	115 (59%)	78 (53%)	0.44
APOE-ε4 (%)	37 (19%)	83 (57%)	**< 0.001**
Aβ PET (Centiloids)	4.9 (11.0)	71.2 (59.0)	**< 0.001**
CSF $Aβ_{42}$	1421 (817)	653 (377)	**< 0.001**
CSF $Aβ_{40}$	18,440 (7680)	17,770 (6150)	0.56
CSF pTau	17.8 (8.2)	27.2 (19.9)	**< 0.001**
CSF pTau/$Aβ_{40}$	0.0010 (0.0002)	0.0016 (0.0009)	**< 0.001**
FTP SUVR (Temporal-metaROI)	1.16 (0.08)	1.28 (0.27)	**< 0.001**
aHCV (mm^3)	7530 (1469)	6990 (1750)	**< 0.001**
PACC	0.25 (5.06)	−2.33 (11.64)	**< 0.001**
116 participants with ≥ 2 tau PET scans			
Sample size	41 (35%)	75 (65%)	
CU/MCI/AD	26/14/1	39/25/11	
FTP visits (median (IQR, range), no.)	2.0 (1.0, 2–4)	2.0 (1.0, 2–4)	
FTP follow-up (Median (IQR, range), years)	1.8 (1.1, 0.8–3.3)	1.2 (1.0, 0.7–3.1)	
139 participants with ≥ 2 aHCV data			
Sample size	64 (46%)	75 (54%)	
CU/MCI/AD	42/20/2	39/24/12	
MRI visits (median (IQR, range), no.)	2.0 (0, 2–4)	2.0 (0.5, 2–4)	
MRI follow-up (median (IQR, range), years)	2.0 (1.0, 0.9–3.8)	1.2 (0.9, 0.8–3.2)	
202 participants with ≥ 2 PACC measurements			
Sample size	99 (49%)	103 (51%)	
CU/MCI/AD	60/37/2	49/36/18	
PACC visits (median (IQR, range), no.)	2 (0, 2–4)	2 (1, 2–5)	
PACC follow-up (median (IQR, range), years)	2.0 (1.0, 0.9–3.0)	1.1 (1.0, 0.7–4.0)	

Abbreviations: *Aβ* amyloid-β, *AD* Alzheimer's disease, *aHCV* adjusted hippocampal volume, *CU* cognitively unimpaired, *FTP* ^{18}F-flortaucipir, *IQR* interquartile range, *MCI* mild cognitive impairment, *PACC* Preclinical Alzheimer Cognitive Composite, *pTau* phosphorylated tau, *SUVR* standardized uptake value ratio

Notably, the association with Aβ PET increased from rho value 0.51 when using CSF pTau alone to 0.67 using the CSF pTau/$Aβ_{40}$ (Fig. 2a, b). Likewise, the association with tau PET increased from rho value 0.43 when using CSF pTau alone to 0.46 using the CSF pTau/$Aβ_{40}$ (Fig. 2c, d). We also compared CSF pTau and CSF pTau/$Aβ_{40}$ in terms of their associations with other measures of neurodegeneration biomarkers and cognition in order to further investigate the validity of CSF pTau/$Aβ_{40}$. CSF pTau/$Aβ_{40}$ but not CSF pTau was negatively associated with baseline aHCV (Fig. 2e, f), and the association with aHCV slope increased from rho value − 0.18 when using CSF pTau alone to − 0.38 using the CSF pTau/$Aβ_{40}$ (Fig. 2g, h). The association with baseline PACC and PACC slope increased from rho values − 0.33 and − 0.24 when using CSF pTau alone to − 0.45 and − 0.39 using the CSF pTau/$Aβ_{40}$ respectively (Fig. 2i, l).

Based on these findings, CSF pTau/$Aβ_{40}$ was used to represent tauopathy in CSF instead of CSF pTau for all subsequent analyses.

We also found that CSF pTau and CSF pTau/$Aβ_{40}$ were both more strongly associated with Aβ PET than they were with tau PET (Fig. 2a–d).

Regions with significant associations between CSF pTau/$Aβ_{40}$ and tau PET

CSF pTau/$Aβ_{40}$ was significantly associated with tau PET SUVRs in all the 35 ROIs, and the strongest

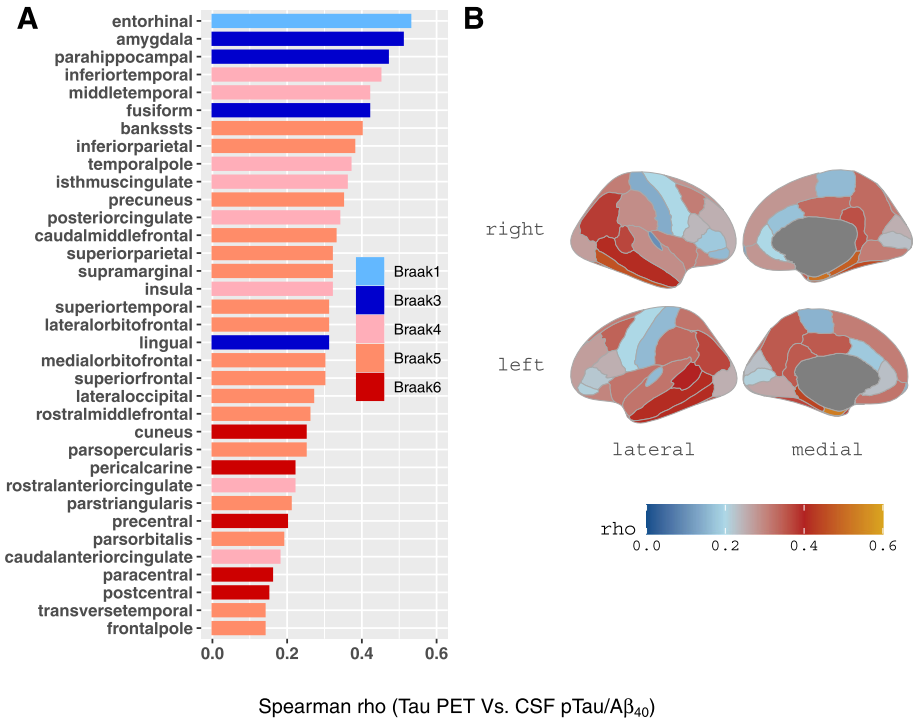

Fig. 3 Regions with significant association between CSF pTau/$A\beta_{40}$ and tau PET. **a** Correlation coefficients between CSF pTau/$A\beta_{40}$ and tau PET SUVRs in Freesurfer-defined regions were illustrated in **a** bar graph and **b** brain map. Abbreviations: Aβ = amyloid-β; FTP = ^{18}F-flortaucipir; pTau = phosphorylated tau; Spearman R = Spearman's correlation coefficient; SUVR = standardized uptake value ratio

association regions were within the Temporal-metaROI region (Fig. 3). We repeated these analyses in Aβ−, Aβ+, CU, and non-demented (CU and MCI) participants. The results were similar for Aβ+ participants (supplemental Fig. 10A), whereas no association was found for Aβ− participants. Similar features were observed for CU and non-demented (CU and MCI) participants (supplemental Fig. 10B-C). Because the strongest associations between CSF pTau/$A\beta_{40}$ and tau PET were within the Temporal-metaROI (Fig. 3), which has been commonly used to detect tau deposition in brain [40–46], temporal tau PET (Temporal-metaROI FTP SUVR) was selected to represent tau deposition for further analyses unless otherwise noted.

Cross-sectional associations between Aβ PET, CSF pTau/$A\beta_{40}$, and tau PET

We found Aβ PET was significantly associated with CSF and PET tau measurements, which were driven by Aβ+ individuals. Baseline Aβ PET was positively associated with CSF pTau (Fig. 4a, $\beta_{std} = 0.32$ [95% CI, 0.15, 0.48]), CSF pTau/$A\beta_{40}$ (Fig. 4b, $\beta_{std} = 0.43$ [95% CI, 0.28, 0.58]), and tau PET in Temporal-metaROI (Fig. 4c, $\beta_{std} = 0.34$ [95% CI, 0.21, 0.48]) and entorhinal (Supplemental Fig. 11A, $\beta_{std} = 0.36$ [95% CI, 0.23, 0.48]) in Aβ+ participants. Notably, the association with Aβ PET increased from rho value 0.38 when using CSF pTau alone to 0.60 using the CSF pTau/$A\beta_{40}$ (Fig. 4a). In Aβ− participants, Aβ PET was weakly but significantly associated with tau PET in entorhinal (Supplemental Fig. 11A, $\beta_{std} = 0.17$ [95% CI, 0.02, 0.33]).

In order to investigate the prevalence of abnormal CSF pTau, CSF pTau/$A\beta_{40}$, and tau PET (entorhinal or Temporal-metaROI), Aβ− and Aβ+ participants were classified as tau normal (T−)/abnormal (T+) using CSF pTau or CSF pTau/$A\beta_{40}$ or tau PET thresholds, dividing the whole cohort into A−/T−, A−/T+, A+/T−, and A+/T+ groups. Few Aβ− participants had abnormal CSF pTau/$A\beta_{40}$ (7.6%) and temporal tau PET (5.3%), whereas Aβ+ participants showed a 3.0–4.5 times higher percentage of abnormal CSF pTau/$A\beta_{40}$ (32.6%) and temporal tau PET (24.0%) than Aβ− participants (Fig. 4b, c). Among Aβ− participants, abnormal CSF pTau had 1.66 times (12.6% vs. 7.6%) higher prevalence than abnormal CSF pTau/$A\beta_{40}$ (Fig. 4a, b). The results were similar for entorhinal tau PET (Supplemental Fig. 11A).

In order to determine the concordance between CSF pTau and CSF pTau/$A\beta_{40}$, and between CSF and PET measures of tau, participants were classified as normal (−)/abnormal (+) on CSF pTau or CSF pTau/$A\beta_{40}$ (PTAU+/−) and entorhinal or Temporal-metaROI FTP SUVR (FTP+/−). Abnormal CSF pTau only had higher prevalence (Fig. 4e, 13.8% vs. 5.1%, odds ratio =

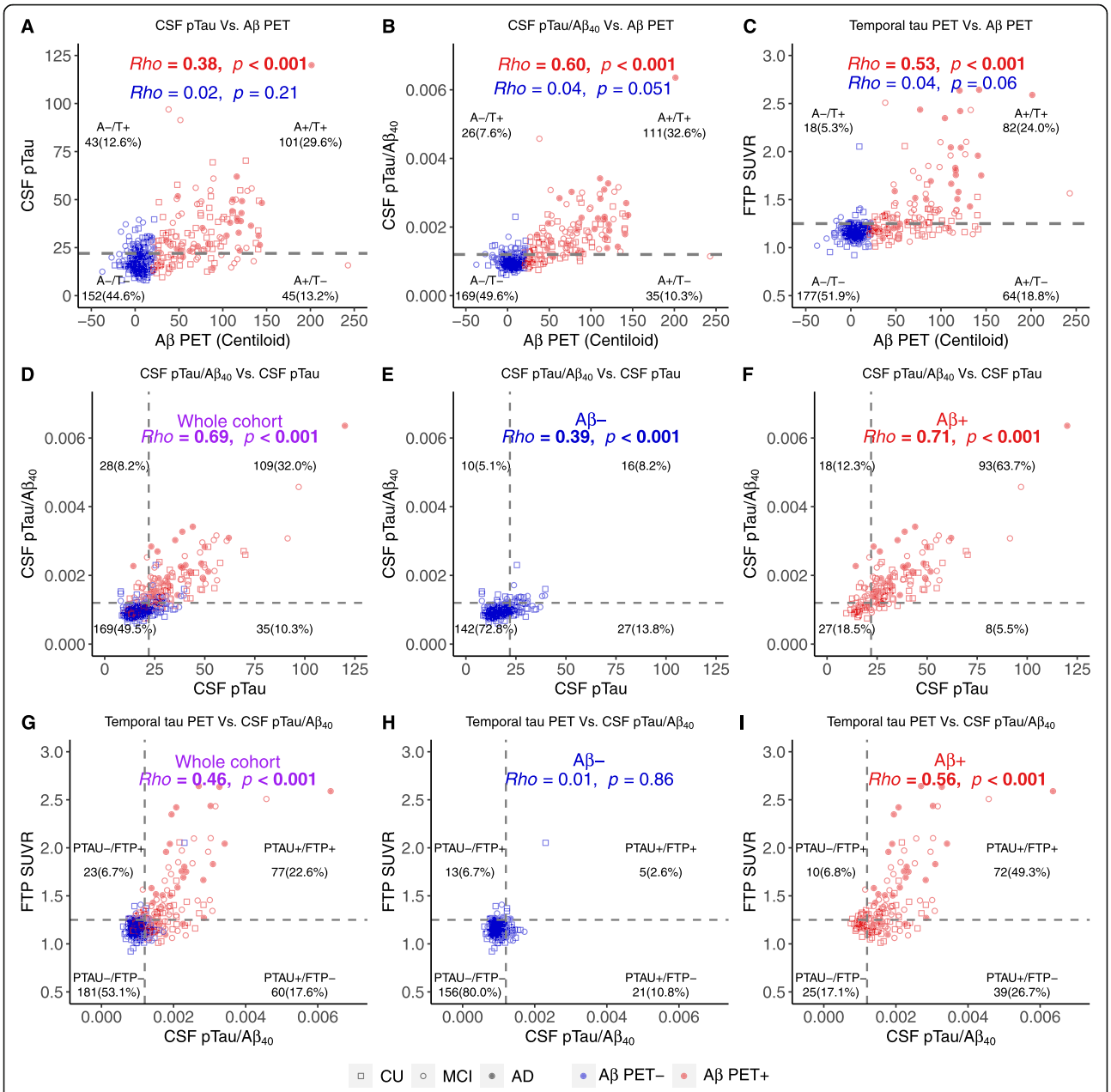

Fig. 4 Cross-sectional associations between Aβ PET, CSF pTau/Aβ$_{40}$, and tau PET. Associations between baseline Aβ PET and **a** CSF pTau, **b** CSF pTau/Aβ$_{40}$, and **c** temporal tau PET. Associations between baseline CSF pTau and CSF pTau/Aβ$_{40}$ in the whole cohort (**d**), Aβ− (**e**), and Aβ+ (**f**) participants. Associations between baseline CSF pTau/Aβ$_{40}$ and Temporal-metaROI tau PET in the whole cohort (**g**), Aβ− (**h**), and Aβ+ (**i**) participants. The vertical and horizontal gray dashed lines reflect the abnormal thresholds of corresponding biomarkers in the *x*-axis and *y*-axis respectively. Abbreviations: Aβ = amyloid-β; A = Aβ PET; − = negative; + = positive; AD = Alzheimer's disease; CU = cognitively unimpaired; FTP = ^{18}F-flortaucipir; MCI = mild cognitive impairment; pTau = phosphorylated tau; PTAU = CSF pTau or CSF pTau/Aβ$_{40}$ ratio; SUVR = standardized uptake value ratio; T = CSF pTau or CSF pTau/Aβ$_{40}$ or tau PET

2.7[95%CI, 1.3–6.3], $p = 0.008$) than abnormal CSF pTau/Aβ$_{40}$ only in Aβ− participants, whereas abnormal CSF pTau/Aβ$_{40}$ only had marginally higher prevalence (Fig. 4f, 12.3% vs. 5.5%, odds ratio = 2.3[95%CI, 0.9–6.0], $p = 0.08$) than abnormal CSF pTau only in Aβ+ participants. CSF pTau/Aβ$_{40}$ (Fig. 4g, $\beta_{std} = 0.59$ [95% CI, 0.51, 0.68]) were positively associated with temporal tau PET across all participants. Aβ+ participants were responsible for this relationship because no association was found in Aβ− participants (Fig. 4h, i). We found that in Aβ− participants, the proportion of participants with abnormal CSF pTau/Aβ$_{40}$ only was comparable to those with an abnormal temporal

tau PET only (10.8% vs. 6.7%) (Fig. 4h). In contrast, in Aβ+ participants, those with abnormal CSF pTau/$A\beta_{40}$ only were fourfold more prevalent than the abnormal temporal tau PET only (Fig. 4i, 26.7% vs. 6.8%, odds ratio = 3.9[95%CI, 1.9–8.8], $p < 0.001$). The results were similar for entorhinal tau PET (Supplemental Fig. 11B-D).

The conservative cutoffs of CSF pTau, CSF pTau/$A\beta_{40}$, entorhinal tau PET, and temporal tau PET were higher and defined fewer "T+" individuals, while the results of concordance of different biomarkers were substantially the same as the initial cutoffs (Supplemental Figs. 12–13).

Associations between Aβ PET, CSF pTau/$A\beta_{40}$, tau PET and longitudinal tau PET change

Baseline Aβ PET (Fig. 5a, $\beta_{std} = 0.42$ [95% CI, 0.22, 0.63]), CSF pTau/$A\beta_{40}$ (Fig. 5b, $\beta_{std} = 0.61$ [95% CI, 0.43, 0.79]), and Temporal-metaROI tau PET (Fig. 5c, $\beta_{std} = 0.63$ [95% CI, 0.45, 0.81]) were all associated with subsequent tau PET increase (ΔFTP) in Aβ+ participants (Fig. 5a–c). In contrast, no predictive effect was found in Aβ− participants.

The latent variable model demonstrated that the direct association between Aβ and ΔFTP increase in Aβ+ participants was not significant after including the CSF pTau/$A\beta_{40}$ and FTP (Fig. 5d), reducing the β value from 0.47 to 0.04 (91% change). CSF pTau/$A\beta_{40}$-involved pathways (pathway1: from Aβ PET to CSF pTau/$A\beta_{40}$ to ΔFTP; pathway2: from Aβ PET to CSF pTau/$A\beta_{40}$ to FTP to ΔFTP) explained 70% of the association (total effect) between Aβ PET and ΔFTP increase in Aβ+ participants.

Prediction of longitudinal cognitive decline

Baseline Aβ PET (Fig. 6a, $\beta_{std} = -0.41$ [95% CI, −0.59, −0.23]), CSF pTau/$A\beta_{40}$ (Fig. 6b, $\beta_{std} = -0.53$ [95% CI, −0.69, −0.36]), and Temporal-metaROI tau PET (Fig. 6c, $\beta_{std} = -0.73$ [95% CI, −0.86, −0.60]) were all associated

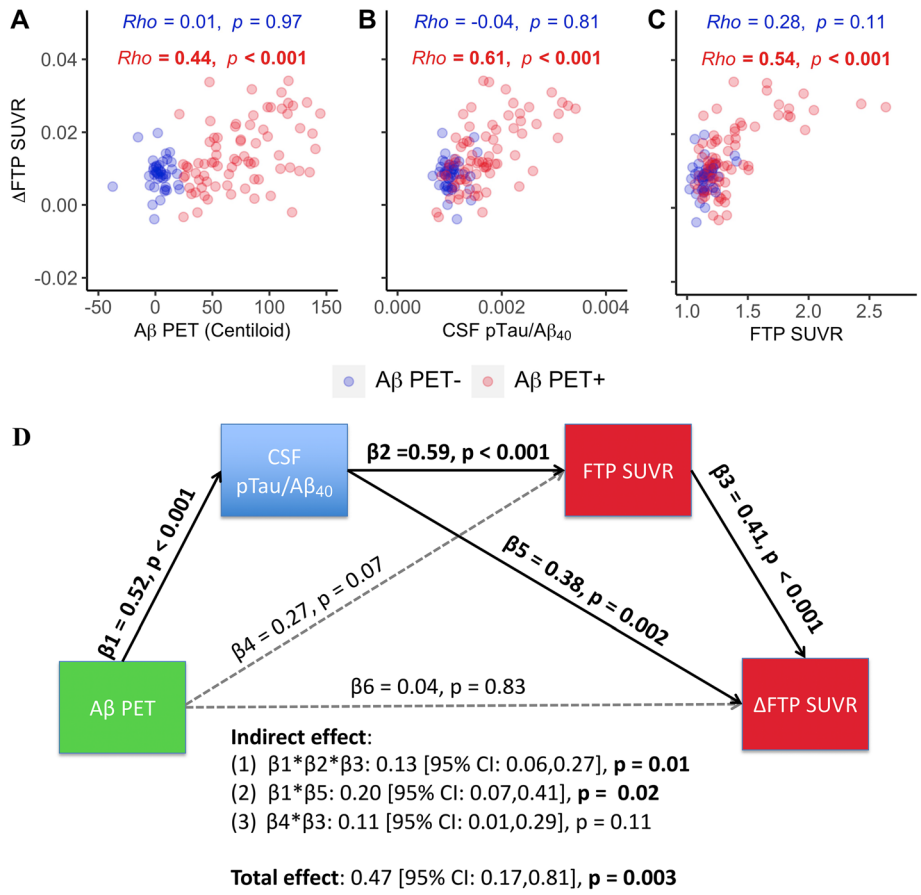

Fig. 5 Associations between baseline Aβ PET, CSF pTau/$A\beta_{40}$, tau PET and longitudinal tau PET change. Associations between annual temporal tau PET change (ΔFTP SUVR in Temporal-metaROI) and **a** baseline Aβ PET, **b** CSF pTau/$A\beta_{40}$, and **c** Temporal-metaROI tau PET (FTP SUVR in Temporal-metaROI). **d** All the possible pathways between Aβ PET, CSF pTau/$A\beta_{40}$, FTP, and ΔFTP were calculated in a serial mediation model in Aβ+ participants. Aβ PET, CSF pTau/$A\beta_{40}$, FTP, and ΔFTP were converted to standard *z* scores. Total, direct, and indirect associations were calculated via a 5000-iteration bootstrapping procedure. Abbreviations: Aβ = amyloid-β; FTP = ^{18}F-flortaucipir; pTau = phosphorylated tau; SUVR = standardized uptake value ratio

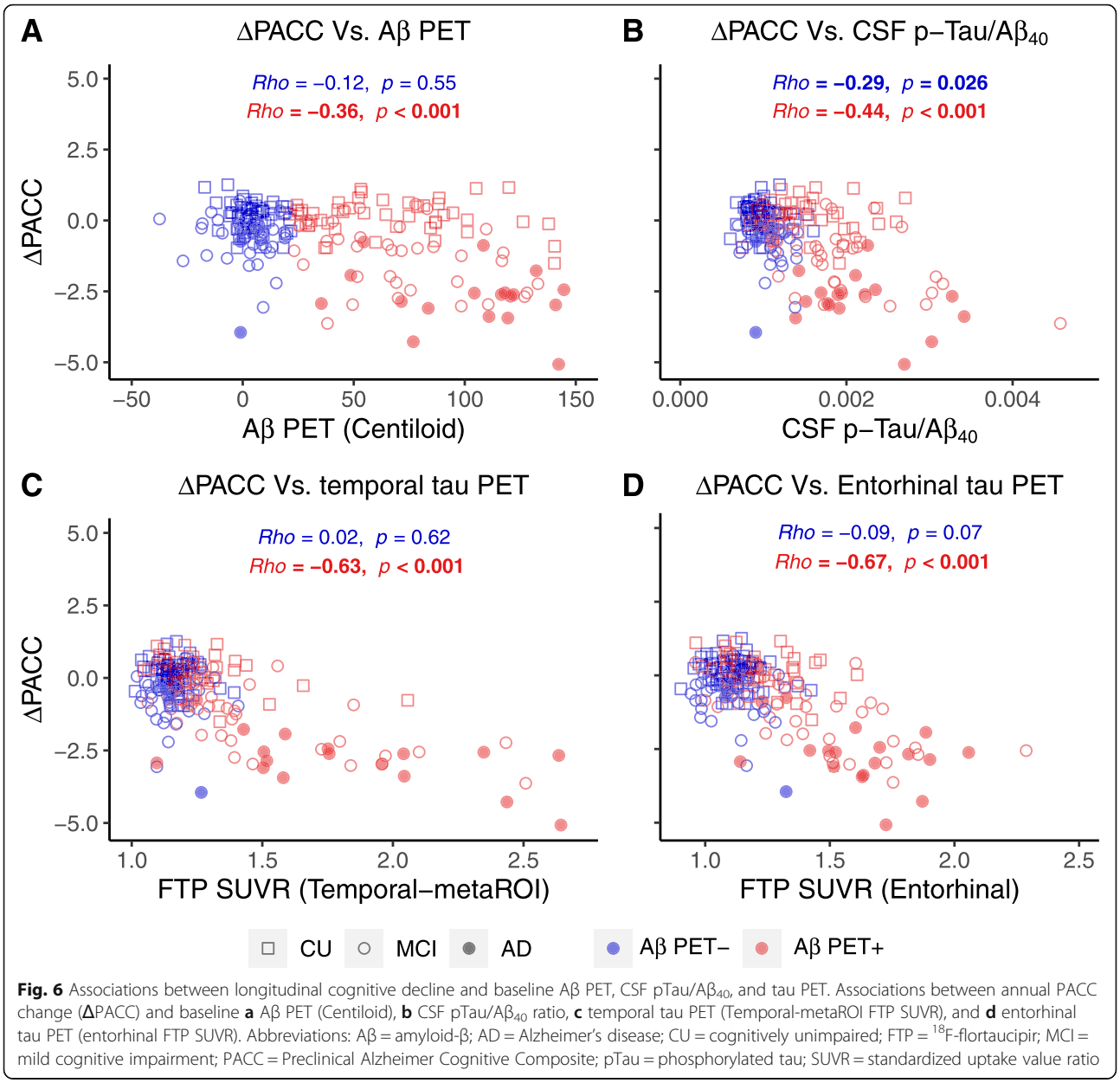

Fig. 6 Associations between longitudinal cognitive decline and baseline Aβ PET, CSF pTau/$Aβ_{40}$, and tau PET. Associations between annual PACC change (ΔPACC) and baseline **a** Aβ PET (Centiloid), **b** CSF pTau/$Aβ_{40}$ ratio, **c** temporal tau PET (Temporal-metaROI FTP SUVR), and **d** entorhinal tau PET (entorhinal FTP SUVR). Abbreviations: Aβ = amyloid-β; AD = Alzheimer's disease; CU = cognitively unimpaired; FTP = ^{18}F-flortaucipir; MCI = mild cognitive impairment; PACC = Preclinical Alzheimer Cognitive Composite; pTau = phosphorylated tau; SUVR = standardized uptake value ratio

with subsequent cognitive decline in Aβ+ participants (Fig. 6), whereas only tau PET (β_{std} = − 0.68[95% CI, − 0.87, − 0.48], $p <$ 0.001) remained predictive when all variables were added into one multivariate model. The results were similar for entorhinal tau PET. In contrast, only CSF pTau/$Aβ_{40}$ (β_{std} = − 0.22[95% CI, − 0.42, − 0.03], p = 0.03) was associated with subsequent cognitive decline in Aβ− participants.

Discussion

This study had several primary findings: (1) use of a CSF pTau/$Aβ_{40}$ ratio reduced noise in pTau likely introduced by individual variability in CSF production rates, and increased associations with Aβ PET, tau PET, hippocampal volume, and cognition compared with CSF pTau alone. (2) Tau PET associations with CSF pTau/$Aβ_{40}$ were highest in medial and lateral temporal regions. (3) Associations between Aβ PET, CSF pTau/$Aβ_{40}$, and tau PET (cross-sectionally and longitudinally) were substantially driven by Aβ PET-positive individuals. (4) Among these Aβ+ individuals, most participants (66%) were concordant on CSF pTau/$Aβ_{40}$ and Temporal-metaROI tau PET, but among discordant individuals, those with abnormal CSF pTau/$Aβ_{40}$ and normal tau PET were 4 times more prevalent (26.7%) than those with abnormal tau PET and normal CSF pTau/$Aβ_{40}$ (6.8%). (5) Among these Aβ+ individuals, baseline Aβ PET, CSF pTau/$Aβ_{40}$, and tau PET were all associated with subsequent tau PET increase, while CSF

pTau/$A\beta_{40}$ significantly mediates the association between Aβ PET and tau PET (cross-sectionally and longitudinally). (6) Only tau PET was predictive of longitudinal cognitive decline when baseline Aβ PET, CSF pTau/Aβ40, and tau PET were put in one multivariate model.

Our motivation to adjust CSF pTau measurements was based on our observation that Aβ PET-negative individuals had abnormal ("positive") CSF pTau that correlated positively with high ("normal") CSF $A\beta_{42}$ (Fig. 1c), suggesting that these elevated measurements reflect high CSF total production rate but not abnormal tau. Similar patterns of elevated pTau and CSF $A\beta_{42}$ in the negative range that are presumably artifactual have been observed in other recent studies from ADNI, BIOFINDER, and Washington University [7, 16], and with CSF data analyzed with mass spectrometry (Supplementary Fig. 9) and immunoassays. CSF pTau/$A\beta_{40}$ appears to be a compelling strategy for improving sensitivity to CSF tau pathology, since this approach reversed the biologically implausible association between CSF pTau and $A\beta_{42}$ and improved associations with downstream markers of AD progression compared with CSF pTau alone. Because CSF $A\beta_{40}$ was not associated with PET measures of either Aβ or tau (Fig. 1a, b) and is not elevated in AD [21–29], its use as a normalization variable is unlikely to bias estimates of CSF pTau. This strategy is in line with recent work supporting use of CSF $A\beta_{42}/A\beta_{40}$ instead of CSF $A\beta_{42}$ alone [6, 7, 17–19], and use of CSF pTau/tTau instead of CSF pTau [47]. However, our results did not exclude other possibilities for the enhanced associations between CSF pTau/$A\beta_{40}$ and downstream markers of AD progression. For example, a few studies [48–51] have reported that CSF $A\beta_{40}$ may decrease in cognitively impaired individuals, which may thereby increase the CSF pTau/$A\beta_{40}$ ratios of cognitively impaired individuals. In addition, one animal study [52] observed that CSF $A\beta_{40}$ may increase in the earliest phase of Aβ accumulation in mouse models, which may delay the increase of CSF pTau/$A\beta_{40}$ in the preclinical stage of AD. We found only trend-level decreases in CSF $A\beta_{40}$ in Aβ− unimpaired and Aβ+ impaired groups relative to Aβ+ unimpaired individuals (data not shown), but it is possible that early and late changes in CSF $A\beta_{40}$ may contribute to the tau-related effects we observed.

Associations between CSF pTau/$A\beta_{40}$ and tau PET were stronger in ROIs in the temporal lobe than other areas such as frontal and occipital lobes that accumulate tau in later stages of disease [53, 54], consistent with our observation and recent studies [14, 15, 55] that CSF tauopathy is an early marker of tau pathology. The strongest associations were within the medial and lateral temporal regions that overlapped with a tau composite region (Temporal-metaROI) reported previously as well as a "Braak III/IV" like ROI [40, 41, 45, 56]. Notably, the relationship between CSF pTau/$A\beta_{40}$ and tau PET was primarily driven by Aβ PET positivity and less influenced by clinical diagnosis (Supplementary Fig. 10), which could also reflect a greater range of tau pathology in Aβ+ individuals and a stronger relationship between Aβ and tau than between tau and clinical symptoms [57, 58]. Consistent with the present study, Chhatwal et al. [10] reported a significant association between CSF pTau and tau PET in limbic regions of the temporal lobe in CU elderly adults. However, two studies [9, 12] did not find significant association between CSF pTau and tau PET in CU individuals, perhaps due to methodological factors such as sample size and the use of CSF pTau alone rather than the CSF pTau/$A\beta_{40}$ ratio.

Elevated Aβ PET was weakly associated with greater tau (CSF pTau/$A\beta_{40}$ or tau PET) in the Aβ− individuals, which was in line with previous reports [59–62]. However, also consistent with previous studies [42, 63, 64], we found that tau (CSF pTau/$A\beta_{40}$ or tau PET) was rarely (5.3–7.9%) abnormal in the Aβ− range (Fig. 4). Furthermore, baseline Aβ PET, CSF pTau/$A\beta_{40}$, and tau PET were predictive of subsequent tau PET increase in the Aβ+ group only, which is in agreement with recent tau PET studies [40, 65]. Together, these findings suggest that tau is rarely increasing or abnormal when Aβ is absent.

In line with our findings, one recent study [15] also reported that CSF pTau mediated the association between Aβ PET and tau PET, and higher CSF pTau was associated with faster tau PET increase rates in cognitively impaired individuals. Unlike this study, we found baseline tau PET was also related to the tau PET rate. The discrepancy may be explained by the larger sample size and the use of white matter reference for longitudinal tau PET in the present study. In the mediation analyses, two significant CSF pTau/$A\beta_{40}$-linked pathways were identified, which explained 70% of the association between Aβ PET and longitudinal brain tau accumulation among Aβ+ individuals.

Finally, consistent with three recent reports [14, 15, 66], we found that tau PET was more predictive of subsequent cognitive decline than CSF tau among Aβ+ individuals, suggesting brain tau may reflect a later tau stage closer to cognitive decline than CSF tau on the Alzheimer's continuum. Interestingly, previous comparisons of CSF and PET measurements of Aβ were analogous in showing that cognitive decline is more related to Aβ PET than CSF Aβ [1, 3, 67, 68]. We also noticed that higher CSF pTau/$A\beta_{40}$ was significantly related to faster longitudinal cognitive decline in amyloid-negative individuals. No previous studies reported the association between CSF pTau and cognitive decline in amyloid-negative individuals, which should be cautious to interpret this result and may need to be validated in other samples.

This study has several limitations. The CSF pTau/Aβ_{40} threshold was derived from the existing sample of ADNI participants and only pTau$_{181}$ was available in the ADNI sample at this time, so it would be helpful to validate the findings in other samples and with other phosphorylation sites (i.e., pTau$_{217}$ [47, 69]) and tau PET ligands. Furthermore, only 9% (31/341) of the participants in this study were AD patients and the longitudinal observation was of relatively short duration, so it would be helpful to confirm those findings using additional participants and extended longitudinal data. Finally, one possible explanation for the differences we observed between tau PET and CSF pTau measurements is that CSF pTau may reflect Aβ in addition to tau pathology. Our observation that both CSF pTau and CSF pTau/Aβ_{40} had stronger associations with Aβ PET than they did with tau PET (Fig. 2a–d) is consistent with this possibility, but further pathology studies are needed to verify this interpretation.

Conclusions

In summary, we found that the use of a CSF pTau/Aβ_{40} ratio improves the sensitivity to detect CSF tau by adjusting for individual differences in CSF production. Furthermore, although PET and CSF measures of tau are broadly concordant in the majority (76%) of individuals when measured dichotomously, our findings support recent work [14] indicating that CSF and PET measures of tau may not be interchangeable in the A/T/N research framework [70]. Among amyloid-positive individuals, higher tauopathy measured with CSF and PET is related to faster tau accumulation, while tau PET was more predictive of subsequent cognitive decline than CSF tau. Taken together, these findings suggest that the interchangeability of PET and CSF measures of tau likely depends on the goals of the study, the phase of AD being studied, and the clinical characteristics of the population.

Supplementary information

Supplementary information accompanies this paper at https://doi.org/10.1186/s13195-020-00665-8.

Additional file 1: Figure S1. The ROC analysis using the Youden index classifying 280 Aβ- ADNI cognitively unimpaired (CU) participants and 183 Aβ + ADNI MCI and AD patients as the endpoint to define the cutoff ≥1.25 for Temporal-metaROI FTP SUVR. AUC: 0.876 (95%CI, 0.84, 0.912). Among these 463 ADNI participants, 217 (47%) participants were included in the analyses of the manuscript. **Figure S2.** Histograms of Temporal-metaROI FTP SUVRs of (A) all 775 ADNI participants, (B) 280 Aβ- ADNI CU participants and (C) 183 Aβ + ADNI MCI and AD patients with tau PET scan. Red dotted line is the cutoff of Temporal-metaROI FTP SUVR 1.25. **Figure S3.** The ROC analysis using the Youden index classifying 280 Aβ- ADNI CU participants and 183 Aβ + ADNI MCI and AD patients as the endpoint to define the cutoff ≥1.21 for entorhinal FTP SUVR. AUC: 0.891 (95%CI, 0.856, 0.926). **Figure S4.** Histograms of entorhinal FTP SUVRs of (A) all 775 ADNI participants, (B) 280 Aβ- ADNI CU participants and (C) 183 Aβ + ADNI MCI and AD patients with tau PET scan. Red dotted line is the cutoff of entorhinal FTP SUVR 1.21. **Figure S5.** The ROC analysis using the Youden index classifying 320 Aβ- ADNI CU participants and 429 Aβ + ADNI MCI and AD patients as the endpoint to define the cutoff ≥22 for CSF p-Tau. AUC: 0.865 (95%CI, 0.84, 0.89). Among these 749 ADNI participants, 212 (28%) participants were included in the analyses of the manuscript. **Figure S6.** Histograms of CSF p-Tau of (A) all 1534 ADNI participants, (B) 320 Aβ- ADNI CU participants and (C) 429 Aβ + ADNI MCI and AD patients with CSF p-Tau measurement. Red dotted line is the cutoff of CSF p-Tau 22. **Figure S7.** The ROC analysis using the Youden index classifying 169 Aβ- ADNI CU participants and 160 Aβ + ADNI MCI and AD patients as the endpoint to define the cutoff ≥0.0012 for CSF p-Tau/Aβ_{40} ratio. AUC: 0.976 (95%CI, 0.96, 0.99). Among these 329 ADNI participants, 201 (61%) participants were included in the analyses of the manuscript. **Figure S8.** Histograms of CSF p-Tau/Aβ_{40} for (A) all 447 ADNI participants, (B) 169 Aβ- ADNI CU participants and (C) 160 Aβ + ADNI MCI and AD patients with CSF p-Tau/Aβ_{40}. Red dotted line is the 0.0012 cutoff for the CSF p-Tau/Aβ_{40} ratio. **Figure S9.** Cross-sectional associations between CSF MASS Aβ_{42} and CSF p-Tau. The vertical gray dashed line reflects the abnormal threshold of CSF p-Tau. Abbreviations: p-Tau = phosphorylated tau; Aβ = amyloid-β; CU = cognitively unimpaired; MCI = mild cognitive impairment; AD = Alzheimer's disease. **Figure S10.** Regions with significant association between CSF P-tau and FTP tau in (A) Aβ+, (B) CU and (C) non-demented participants. Abbreviations: Spearman rho = Spearman's correlation coefficient; p-Tau = phosphorylated tau; Aβ = amyloid-β; FTP = ^{18}F-flortaucipir; SUVR = standardized uptake value ratio; CU = cognitively unimpaired; MCI = mild cognitive impairment; AD = Alzheimer's disease. **Figure S11.** Cross-sectional associations between Aβ PET, CSF p-Tau/Aβ_{40} and entorhinal tau PET. (A). Associations between baseline entorhinal tau PET and Aβ PET. Associations between baseline CSF p-Tau/Aβ_{40} and entorhinal tau PET in the whole cohort (B), Aβ- (C) and Aβ + (D) participants. The vertical and horizontal gray dashed lines reflect the abnormal thresholds of corresponding biomarkers in x-axis and y-axis respectively. Abbreviations: Aβ = amyloid-β; A = Aβ PET; − = negative; + = positive; AD = Alzheimer's disease; CU = cognitively unimpaired; FTP = ^{18}F-flortaucipir; MCI = mild cognitive impairment. **Figure S12.** Cross-sectional associations between Aβ PET, CSF pTau/Aβ_{40} and tau PET using alternative cutoffs. Associations between baseline Aβ PET and (A) CSF pTau, (B) CSF pTau/Aβ_{40} and (C) temporal tau PET. Associations between baseline CSF pTau and CSF pTau/Aβ_{40} in the whole cohort (D), Aβ- (E) and Aβ + (F) participants. Associations between baseline CSF pTau/Aβ_{40} and Temporal-metaROI tau PET in the whole cohort (G), Aβ- (H) and Aβ + (I) participants. The vertical and horizontal gray dashed lines reflect the abnormal thresholds of corresponding biomarkers in x-axis and y-axis respectively. Abbreviations: Aβ = amyloid-β; A = Aβ PET; − = negative; + = positive; AD = Alzheimer's disease; CU = cognitively unimpaired; FTP = ^{18}F-flortaucipir; MCI = mild cognitive impairment; pTau = phosphorylated tau; PTAU = CSF pTau or CSF pTau/Aβ_{40} ratio; SUVR = standardized uptake value ratio; T = CSF pTau or CSF pTau/Aβ_{40} or tau PET. **Figure S13.** Cross-sectional associations between Aβ PET, CSF p-Tau/Aβ_{40} and entorhinal tau PET using alternative cutoffs. (A). Associations between baseline entorhinal tau PET and Aβ PET. Associations between baseline CSF p-Tau/Aβ_{40} and entorhinal tau PET in the whole cohort (B), Aβ- (C) and Aβ + (D) participants. The vertical and horizontal gray dashed lines reflect the abnormal thresholds of corresponding biomarkers in x-axis and y-axis respectively. Abbreviations: Aβ = amyloid-β; A = Aβ PET; − = negative; + = positive; AD = Alzheimer's disease; CU = cognitively unimpaired; FTP = ^{18}F-flortaucipir; MCI = mild cognitive impairment.

Abbreviations

Aβ: Amyloid-β; ADNI: Alzheimer's Disease Neuroimaging Initiative; β_{std}: Standardized β coefficient; CSF pTau: CSF phosphorylated tau; CU: Cognitively unimpaired; CI: Confidence interval; FTP: ^{18}F-flortaucipir; FBP: ^{18}F-florbetapir; FBB: ^{18}F-florbetaben; GLM: Generalized linear model; MCI: Mild cognitive impairment; PACC: Preclinical Alzheimer Cognitive Composite; ROI: Regions of interest; SNAP: Suspected non-Alzheimer's pathology; SUVR: Standardized uptake value ratio

Acknowledgements

The authors would like to thank Henrik Zetterberg, Kaj Blennow, and Oskar Hansson for their comments on data interpretation, and all the ADNI participants and staff for their contributions to data acquisition. The Data

collection and sharing for this project was funded by the Alzheimer's Disease Neuroimaging Initiative (ADNI) (National Institutes of Health Grant U01 AG024904) and DOD ADNI (Department of Defense award number W81XWH-12-2-0012). ADNI is funded by the National Institute on Aging, the National Institute of Biomedical Imaging and Bioengineering, and through generous contributions from the following: AbbVie, Alzheimer's Association; Alzheimer's Drug Discovery Foundation; Araclon Biotech; BioClinica, Inc.; Biogen; Bristol-Myers Squibb Company; CereSpir, Inc.; Eisai Inc.; Elan Pharmaceuticals, Inc.; Eli Lilly and Company; EuroImmun; F. Hoffmann-La Roche Ltd. and its affiliated company Genentech, Inc.; Fujirebio; GE Healthcare; IXICO Ltd.; Janssen Alzheimer Immunotherapy Research & Development, LLC.; Johnson & Johnson Pharmaceutical Research & Development LLC.; Lumosity; Lundbeck; Merck & Co., Inc.; Meso Scale Diagnostics, LLC.; NeuroRx Research; Neurotrack Technologies; Novartis Pharmaceuticals Corporation; Pfizer Inc.; Piramal Imaging; Servier; Takeda Pharmaceutical Company; and Transition Therapeutics. The Canadian Institutes of Health Research is providing funds to support ADNI clinical sites in Canada. Private sector contributions are facilitated by the Foundation for the National Institutes of Health (www.fnih.org). The grantee organization is the Northern California Institute for Research and Education, and the study is coordinated by the Alzheimer's Disease Cooperative Study at the University of California, San Diego. ADNI data are disseminated by the Laboratory for NeuroImaging at the University of Southern California.
Data used in preparation of this article were obtained from the Alzheimer's Disease Neuroimaging Initiative (ADNI) database (adni.loni.usc.edu). As such, the investigators within the ADNI contributed to the design and implementation of ADNI and/or provided data but did not participate in analysis or writing of this report. A complete listing of ADNI investigators can be found at: http://adni.loni.usc.edu/wp-content/uploads/how_to_apply/ADNI_Acknowledgement_List.pdf.

Authors' contributions
T.G contributed to the study design, drafting and editing of the manuscript, data and statistical analysis, and interpretation of results; D.K contributed to acquiring data and editing the manuscript; R.L contributed to interpretation of results and editing the manuscript. L.M.S. and J.Q.T contributed to acquiring data, interpretation of results, obtaining funding, and editing the manuscript; W.J.J and S.M.L contributed to acquiring data, interpretation of results, obtaining funding, editing the manuscript, and study supervision. The author(s) read and approved the final manuscript.

Funding
Not applicable.

Availability of data and materials
The dataset supporting the conclusions of this article is available in the ADNI repository (ida.loni.usc.edu). Derived data is available from the corresponding author on request by any qualified investigator subject to a data use agreement.

Ethics approval and consent to participate
All procedures performed in studies involving human participants were in accordance with the ethical standards of the institutional and/or national research committee and with the principles of the 1964 Declaration of Helsinki and its later amendments or comparable ethical standards. Formed written consent was obtained from all participants at each site of ADNI.

Consent for publication
Not applicable.

Competing interests
The authors declare that they have no competing interests.

Author details
[1]Helen Wills Neuroscience Institute, University of California, 132 Barker Hall, Berkeley, CA 94720, USA. [2]Molecular Biophysics and Integrated Bioimaging, Lawrence Berkeley National Laboratory, Berkeley, CA, USA. [3]Memory & Aging Center, Department of Neurology, University of California, San Francisco, CA, USA. [4]Department of Pathology and Laboratory Medicine, Perelman School of Medicine, University of Pennsylvania, Philadelphia, PA, USA.

Received: 21 May 2020 Accepted: 4 August 2020
Published online: 15 August 2020

References
1. Mattsson N, Insel PS, Donohue M, Landau S, Jagust WJ, Shaw LM, et al. Independent information from cerebrospinal fluid amyloid-β and florbetapir imaging in Alzheimer's disease. Brain. 2015;138:772–83.
2. Palmqvist S, Mattsson N, Hansson O. Cerebrospinal fluid analysis detects cerebral amyloid-β accumulation earlier than positron emission tomography. Brain. 2016;139:1226–36.
3. Toledo JB, Bjerke M, Da X, Landau SM, Foster NL, Jagust W, et al. Nonlinear association between cerebrospinal fluid and florbetapir F-18 β-amyloid measures across the spectrum of Alzheimer disease. JAMA Neurol. 2015;72:571–81.
4. Vlassenko AG, McCue L, Jasielec MS, Su Y, Gordon BA, Xiong C, et al. Imaging and cerebrospinal fluid biomarkers in early preclinical Alzheimer disease. Ann Neurol. 2016;80:379–87.
5. Racine AM, Koscik RL, Nicholas CR, Clark LR, Okonkwo OC, Oh JM, et al. Cerebrospinal fluid ratios with Aβ 42 predict preclinical brain β-amyloid accumulation. Alzheimer's Dement Diagnosis, Assess Dis Monit. 2016;2:27–38.
6. Leuzy A, Chiotis K, Hasselbalch SG, Rinne JO, De Mendonça A, Otto M, et al. Pittsburgh compound B imaging and cerebrospinal fluid amyloid-β in a multicentre European memory clinic study. Brain. 2016;139:2540–53.
7. Schindler SE, Gray JD, Gordon BA, Xiong C, Batrla-Utermann R, Quan M, et al. Cerebrospinal fluid biomarkers measured by Elecsys assays compared to amyloid imaging. Alzheimer's Dement. 2018;14:1460–9.
8. Korecka M, Figurski MJ, Landau SM, Brylska M, Alexander J, Blennow K, et al. Analytical and clinical performance of amyloid-beta peptides measurements in CSF of ADNIGO/2 participants by an LC–MS/MS reference method. Clin Chem. 2020;30:106–8.
9. Gordon BA, Friedrichsen K, Brier M, Blazey T, Su Y, Christensen J, et al. The relationship between cerebrospinal fluid markers of Alzheimer pathology and positron emission tomography tau imaging. Brain. 2016;139:2249–60.
10. Chhatwal JP, Schultz AP, Marshall GA, Boot B, Gomez-Isla T, Dumurgier J, et al. Temporal T807 binding correlates with CSF tau and phospho-tau in normal elderly. Neurology. 2016;87:920–6.
11. Brier MR, Gordon B, Friedrichsen K, McCarthy J, Stern A, Christensen J, et al. Tau and Aβ imaging, CSF measures, and cognition in Alzheimer's disease. Sci Transl Med. 2016;8:338ra66.
12. Mattsson N, Schöll M, Strandberg O, Smith R, Palmqvist S, Insel PS, et al. 18 F-AV-1451 and CSF T-tau and P-tau as biomarkers in Alzheimer's disease. EMBO Mol Med. 2017;9:1212–23.
13. La Joie R, Bejanin A, Fagan AM, Ayakta N, Baker SL, Bourakova V, et al. Associations between [18 F]AV1451 tau PET and CSF measures of tau pathology in a clinical sample. Neurology. 2018;90:e282–90.
14. Meyer P-F, Pichet Binette A, Gonneaud J, Breitner JCS, Villeneuve S. Characterization of Alzheimer disease biomarker discrepancies using cerebrospinal fluid phosphorylated tau and AV1451 positron emission tomography. JAMA Neurol. 2020;77:508.
15. Mattsson-Carlgren N, Andersson E, Janelidze S, Ossenkoppele R, Insel P, Strandberg O, et al. Aβ deposition is associated with increases in soluble and phosphorylated tau that precede a positive Tau PET in Alzheimer's disease. Sci Adv. 2020;6:eaaz2387.
16. Hansson O, Seibyl J, Stomrud E, Zetterberg H, Trojanowski JQ, Bittner T, et al. CSF biomarkers of Alzheimer's disease concord with amyloid-β PET and predict clinical progression: a study of fully automated immunoassays in BioFINDER and ADNI cohorts. Alzheimers Dement. 2018;14:1470–81.
17. Janelidze S, Pannee J, Mikulskis A, Chiao P, Zetterberg H, Blennow K, et al. Concordance between different amyloid immunoassays and visual amyloid positron emission tomographic assessment. JAMA Neurol. 2017;74:1492–501.
18. Pannee J, Portelius E, Minthon L, Gobom J, Andreasson U, Zetterberg H, et al. Reference measurement procedure for CSF amyloid beta (Aβ)1–42and the CSF Aβ1–42/Aβ1–40ratio – a cross-validation study against amyloid PET. J Neurochem. 2016;139:651–8.
19. Lewczuk P, Matzen A, Blennow K, Parnetti L, Molinuevo JL, Eusebi P, et al. Cerebrospinal fluid Aβ42/40 corresponds better than Aβ42 to amyloid PET in Alzheimer's disease. J Alzheimers Dis. 2017;55:813–22.
20. Portelius E, Westman-Brinkmalm A, Zetterberg H, Blennow K. Determination of β-amyloid peptide signatures in cerebrospinal fluid using Immunoprecipitation-mass spectrometry. J Proteome Res. 2006;5:1010–6.

21. Wiltfang J, Esselmann H, Bibl M, Hüll M, Hampel H, Kessler H, et al. Amyloid β peptide ratio 42/40 but not Aβ42 correlates with phospho-tau in patients with low- and high-CSF Aβ40 load. J Neurochem. 2007;101:1053–9.
22. Janelidze S, Zetterberg H, Mattsson N, Palmqvist S, Vanderstichele H, Lindberg O, et al. CSF Aβ42/Aβ40 and Aβ42/Aβ38 ratios: better diagnostic markers of Alzheimer disease. Ann Clin Transl Neurol. 2016;3:154–65.
23. Kanai M, Matsubara E, Isoe K, Urakami K, Nakashima K, Arai H, et al. Longitudinal study of cerebrospinal fluid levels of tau, a beta1-40, and a beta1-42(43) in Alzheimer's disease: a study in Japan. Ann Neurol. 1998;44:17–26.
24. Shoji M, Matsubara E, Kanai M, Watanabe M, Nakamura T, Tomidokoro Y, et al. Combination assay of CSF tau, Aβ1-40 and Aβ1-42(43) as a biochemical marker of Alzheimer's disease. J Neurol Sci. 1998;158:134–40.
25. Lewczuk P, Esselmann H, Otto M, Maler JM, Henkel AW, Henkel MK, et al. Neurochemical diagnosis of Alzheimer's dementia by CSF Aβ42, Aβ42/Aβ40 ratio and total tau. Neurobiol Aging. 2004;25:273–81.
26. Fagan AM, Mintun MA, Mach RH, Lee S-Y, Dence CS, Shah AR, et al. Inverse relation between in vivo amyloid imaging load and cerebrospinal fluid Aβ 42 in humans. Ann Neurol. 2006;59:512–9.
27. Fagan AM, Roe CM, Xiong C, Mintun MA, Morris JC, Holtzman DM. Cerebrospinal fluid tau/beta-amyloid (42) ratio as a prediction of cognitive decline in nondemented older adults. Arch Neurol. 2007;64:343–9.
28. Fagan AM, Mintun MA, Shah AR, Aldea P, Roe CM, Mach RH, et al. Cerebrospinal fluid tau and ptau181 increase with cortical amyloid deposition in cognitively normal individuals: implications for future clinical trials of Alzheimer's disease. EMBO Mol Med. 2009;1:371–80.
29. Olsson B, Lautner R, Andreasson U, Öhrfelt A, Portelius E, Bjerke M, et al. CSF and blood biomarkers for the diagnosis of Alzheimer's disease: a systematic review and meta-analysis. Lancet Neurol. 2016;15:673–84.
30. Landau SM, Fero A, Baker SL, Koeppe R, Mintun M, Chen K, et al. Measurement of longitudinal -amyloid change with 18F-Florbetapir PET and standardized uptake value ratios. J Nucl Med. 2015;56:567–74.
31. Baker SL, Maass A, Jagust WJ. Considerations and code for partial volume correcting [18 F]-AV-1451 tau PET data. Data Br. 2017;15:648–57.
32. Jack CR, Wiste HJ, Weigand SD, Therneau TM, Lowe VJ, Knopman DS, et al. Defining imaging biomarker cut points for brain aging and Alzheimer's disease. Alzheimers Dement. 2017;13:205–16.
33. Harrison TM, La Joie R, Maass A, Baker SL, Swinnerton K, Fenton L, et al. Longitudinal tau accumulation and atrophy in aging and alzheimer disease. Ann Neurol. 2019;85:229–40.
34. Hanseeuw BJ, Betensky RA, Jacobs HIL, Schultz AP, Sepulcre J, Becker JA, et al. Association of amyloid and tau with cognition in preclinical Alzheimer disease. JAMA Neurol. 2019;76:915.
35. Southekal S, Devous MD, Kennedy I, Navitsky M, Lu M, Joshi AD, et al. Flortaucipir F 18 quantitation using parametric estimation of reference signal intensity. J Nucl Med. 2018;59:944–51.
36. Buckner RL, Head D, Parker J, Fotenos AF, Marcus D, Morris JC, et al. A unified approach for morphometric and functional data analysis in young, old, and demented adults using automated atlas-based head size normalization: reliability and validation against manual measurement of total intracranial volume. Neuroimage. 2004;23:724–38.
37. Bittner T, Zetterberg H, Teunissen CE, Ostlund RE, Militello M, Andreasson U, et al. Technical performance of a novel, fully automated electrochemiluminescence immunoassay for the quantitation of β-amyloid (1–42) in human cerebrospinal fluid. Alzheimers Dement. 2016; 12:517–26.
38. Donohue MC, Sperling RA, Salmon DP, Rentz DM, Raman R, Thomas RG, et al. The preclinical Alzheimer cognitive composite: measuring amyloid-related decline. JAMA Neurol. 2014;71:961–70.
39. Rosseel Y. Lavaan : an R package for structural equation modeling. J Stat Softw. 2012;48:1–93.
40. Jack CR, Wiste HJ, Schwarz CG, Lowe VJ, Senjem ML, Vemuri P, et al. Longitudinal tau PET in ageing and Alzheimer's disease. Brain. 2018;141: 1517–28.
41. Jack CR, Wiste HJ, Therneau TM, Weigand SD, Knopman DS, Mielke MM, et al. Associations of amyloid, tau, and neurodegeneration biomarker profiles with rates of memory decline among individuals without dementia. JAMA. 2019;321:2316.
42. Jack CR, Wiste HJ, Botha H, Weigand SD, Therneau TM, Knopman DS, et al. The bivariate distribution of amyloid-β and tau: relationship with established neurocognitive clinical syndromes. Brain. 2019;142:3230–42.
43. Park J-C, Han S-H, Yi D, Byun MS, Lee JH, Jang S, et al. Plasma tau/amyloid-β1–42 ratio predicts brain tau deposition and neurodegeneration in Alzheimer's disease. Brain. 2019;142:771–86.
44. Graff-Radford J, Arenaza-Urquijo EM, Knopman DS, Schwarz CG, Brown RD, Rabinstein AA, et al. White matter hyperintensities: relationship to amyloid and tau burden. Brain. 2019;142:2483–91.
45. Botha H, Mantyh WG, Graff-Radford J, Machulda MM, Przybelski SA, Wiste HJ, et al. Tau-negative amnestic dementia masquerading as Alzheimer disease dementia. Neurology. 2018;90:e940–6.
46. Ossenkoppele R, Rabinovici GD, Smith R, Cho H, Schöll M, Strandberg O, et al. Discriminative accuracy of [18 F] flortaucipir positron emission tomography for Alzheimer disease vs other neurodegenerative disorders. JAMA. 2018;320:1151.
47. Janelidze S, Stomrud E, Smith R, Palmqvist S, Mattsson N, Airey DC, et al. Cerebrospinal fluid p-tau217 performs better than p-tau181 as a biomarker of Alzheimer's disease. Nat Commun. 2020;11:1683.
48. Slaets S, Le Bastard N, Martin JJ, Sleegers K, Van Broeckhoven C, De Deyn PP, et al. Cerebrospinal fluid Abeta1-40 improves differential dementia diagnosis in patients with intermediate P-tau181P levels. J Alzheimers Dis. 2013;36:759–67.
49. Mattsson N, Portelius E, Rolstad S, Gustavsson M, Andreasson U, Stridsberg M, et al. Longitudinal cerebrospinal fluid biomarkers over four years in mild cognitive impairment. J Alzheimers Dis. 2012;30:767–78.
50. Jensen M, Schröder J, Blomberg M, Engvall B, Pantel J, Ida N, et al. Cerebrospinal fluid Aβ42 is increased early in sporadic Alzheimer's disease and declines with disease progression. Ann Neurol. 1999;45:504–11.
51. Tapiola T, Pirttilä T, Mikkonen M, Mehta PD, Alafuzoff I, Koivisto K, et al. Three-year follow-up of cerebrospinal fluid tau, β-amyloid 42 and 40 concentrations in Alzheimer's disease. Neurosci Lett. 2000;280:119–22.
52. Maia LF, Kaeser SA, Reichwald J, Lambert M, Obermuller U, Schelle J, et al. Increased CSF a during the very early phase of cerebral a deposition in mouse models. EMBO Mol Med. 2015;7:895–903.
53. Braak H, Braak E. Neuropathological stageing of Alzheimer-related changes. Acta Neuropathol. 1991;82:239–59.
54. Cho H, Choi JY, Hwang MS, Kim YJ, Lee HM, Lee HS, et al. In vivo cortical spreading pattern of tau and amyloid in the Alzheimer disease spectrum. Ann Neurol. 2016;80:247–58.
55. Barthélemy NR, Li Y, Joseph-Mathurin N, Gordon BA, Hassenstab J, Benzinger TLS, et al. A soluble phosphorylated tau signature links tau, amyloid and the evolution of stages of dominantly inherited Alzheimer's disease. Nat Med. 2020;26:398–407.
56. Maass A, Landau S, Baker SL, Horng A, Lockhart SN, La Joie R, et al. Comparison of multiple tau-PET measures as biomarkers in aging and Alzheimer's disease. Neuroimage. 2017;157:448–63.
57. Jagust W, Jack CR, Bennett DA, Blennow K, Haeberlein SB, Holtzman DM, et al. "Alzheimer's disease" is neither "Alzheimer's clinical syndrome" nor "dementia." Alzheimers Dement 2019;15:153–157.
58. Jack CR, Therneau TM, Weigand SD, Wiste HJ, Knopman DS, Vemuri P, et al. Prevalence of biologically vs clinically defined Alzheimer spectrum entities using the National Institute on Aging–Alzheimer's Association Research Framework. JAMA Neurol. 2019;76:1174.
59. Leal SL, Lockhart SN, Maass A, Bell RK, Jagust WJ. Subthreshold amyloid predicts tau deposition in aging. J Neurosci. 2018;38:0485–18.
60. Tosun D, Landau S, Aisen PS, Petersen RC, Mintun M, Jagust W, et al. Association between tau deposition and antecedent amyloid-β accumulation rates in normal and early symptomatic individuals. Brain. 2017;140:1499–512.
61. Palmqvist S, Insel PS, Stomrud E, Janelidze S, Zetterberg H, Brix B, et al. Cerebrospinal fluid and plasma biomarker trajectories with increasing amyloid deposition in Alzheimer's disease. EMBO Mol Med. 2019;e11170.
62. Guo T, Landau SM, Jagust WJ. Detecting earlier stages of amyloid deposition using PET in cognitively normal elderly adults. Neurology. 2020;94:e1512–24.
63. Pontecorvo MJ, Devous MD, Navitsky M, Lu M, Salloway S, Schaerf FW, et al. Relationships between flortaucipir PET tau binding and amyloid burden, clinical diagnosis, age and cognition. Brain. 2017;140:aww334.
64. Guo T, Korman D, Baker SL, Landau SM, Jagust WJ. Longitudinal cognitive and biomarker measurements support a unidirectional pathway in Alzheimer's Disease pathophysiology. Biol Psychiatry. 2020;. https://doi.org/10.1016/j.biopsych.2020.06.029.
65. Pontecorvo MJ, Devous MD, Kennedy I, Navitsky M, Lu M, Galante N, et al. A multicentre longitudinal study of flortaucipir (18F) in normal ageing, mild

cognitive impairment and Alzheimer's disease dementia. Brain. 2019;142: 1723–35.
66. Wolters EE, Ossenkoppele R, Verfaillie SCJ, Coomans EM, Timmers T, Visser D, et al. Regional [18F] flortaucipir PET is more closely associated with disease severity than CSF p-tau in Alzheimer's disease. Eur J Nucl Med Mol Imaging. 2020;. https://doi.org/10.1007/s00259-020-04758-2.
67. Palmqvist S, Zetterberg H, Blennow K, Vestberg S, Andreasson U, Brooks DJ, et al. Accuracy of brain amyloid detection in clinical practice using cerebrospinal fluid β-amyloid 42: a cross-validation study against amyloid positron emission tomography. JAMA Neurol. 2014;71:1282–9.
68. Guo T, Shaw LM, Trojanowski JQ, Jagust WJ, Landau SM. Association of CSF Aβ, amyloid PET and cognition in cognitively unimpaired elderly adults. Neurology. 2020;. https://doi.org/10.1212/WNL.0000000000010596.
69. Barthélemy NR, Bateman RJ, Hirtz C, Marin P, Becher F, Sato C, et al. Cerebrospinal fluid phospho-tau T217 outperforms T181 as a biomarker for the differential diagnosis of Alzheimer's disease and PET amyloid-positive patient identification. Alzheimers Res Ther. 2020;12:26.
70. Jack CR, Bennett DA, Blennow K, Carrillo MC, Dunn B, Haeberlein SB, et al. NIA-AA research framework: toward a biological definition of Alzheimer's disease. Alzheimers Dement. 2018;14:535–62.

Publisher's Note

Springer Nature remains neutral with regard to jurisdictional claims in published maps and institutional affiliations.

Ready to submit your research? Choose BMC and benefit from:

- fast, convenient online submission
- thorough peer review by experienced researchers in your field
- rapid publication on acceptance
- support for research data, including large and complex data types
- gold Open Access which fosters wider collaboration and increased citations
- maximum visibility for your research: over 100M website views per year

At BMC, research is always in progress.

Learn more biomedcentral.com/submissions

BMC